Multimode nematicon waveguides

Yana V. Izdebskaya,[1,*] Anton S. Desyatnikov,[1] Gaetano Assanto,[2] and Yuri S. Kivshar[1]

[1]*Nonlinear Physics Center, Research School of Physics and Engineering, The Australian National University, Canberra, Australian Capital Territory 0200, Australia*

[2]*NooEL–Nonlinear Optics and OptoElectronics Lab, Department of Electronic Engineering, University of Rome "Roma Tre," 00146 Rome, Italy*

**Corresponding author: yvi124@rsphysse.anu.edu.au*

Received October 25, 2010; accepted November 26, 2010;
posted December 8, 2010 (Doc. ID 137028); published January 11, 2011

We report on the first (to our knowledge) experimental observation of higher-order modes guided by soliton-induced waveguides in nematic liquid crystals. We find that the nematicon waveguides operate in a bounded power region specific to each guided mode. Below this region, the guided beams diffract; above this region, the mode mixing and coupling give rise to an unstable output.

OCIS codes: 190.0190, 190.5940, 190.6135.

Spatial optical solitons propagate in nonlinear Kerr-like media as modes of self-induced waveguides [1]. An attractive property of soliton-induced waveguides is their ability to guide weak signals of different wavelengths [2–4], as well as the possibility to reconfigure such waveguides by spatial steering [4–7].

Another dimension in soliton-based optical switching is offered by the multimodal character of self-induced waveguides, observed earlier with photorefractive solitons [2,8]. In this regard, the *nematicon* waveguides, i.e., those induced by spatial optical solitons in nematic liquid crystals (NLCs) [3,5,6], are of particular interest because of the long-range or highly nonlocal character of the reorientational nonlinearity. The transverse size of the nematicon-induced index perturbation can be up to 1 order of magnitude larger than the beam itself [9–11], and therefore such a waveguide is expected to be multimoded. Additional evidence of such multimodality is the existence of higher-order nonlocal solitons [12,13] and incoherent solitons [14,15]. To date, the higher-order modes guided by fundamental nematicons were never observed.

In this Letter we study experimentally the multimode soliton waveguides in NLCs, identifying the power domains where high-order guided modes are supported. These domains are limited from above, because the number of modes grows with nematicon power, whereas their mixing eventually gives rise to unstable outputs. The cell geometry and finite size sets additional limits to the order and orientation of nematicon-guided modes. Because of liquid crystal birefringence, the distinction between hybrid EH and HE modes is not possible [16], and we use the notation H_{mn} or Hermite-like modes with indices (m, n).

The experimental setup is shown in Fig. 1(a). We employ a planar cell with the (propagation) length of 1.1 mm, formed by two $L = 100$ μm spaced parallel polycarbonate slides containing the 6CHBT NLC. The mean angular orientation of the NLC molecules (the molecular *director*) was preset by mechanically rubbing the internal interfaces at $\pi/4$ angle with respect to z in the $(x$–$z)$ plane, parallel to the slides. To prevent the formation of exposed menisci, two additional 150-μm-thick slides were attached perpendicularly to z to seal the cell input and output. We use micro-objectives and CCD cameras to collect the light at the sample output and scattered above the cell during propagation.

Figures 1(b) and 1(c) show sample top-view photos of either ordinary (o, electric field parallel to y) or extraordinary (e, electric field parallel to x) polarized green beams ($\lambda_1 = 532$ nm) launched with 2 mW input power and the wavevector $\mathbf{k}$ aligned to z. Clearly, the o beam in Fig. 1(b) diffracts below the Fréedericksz threshold,

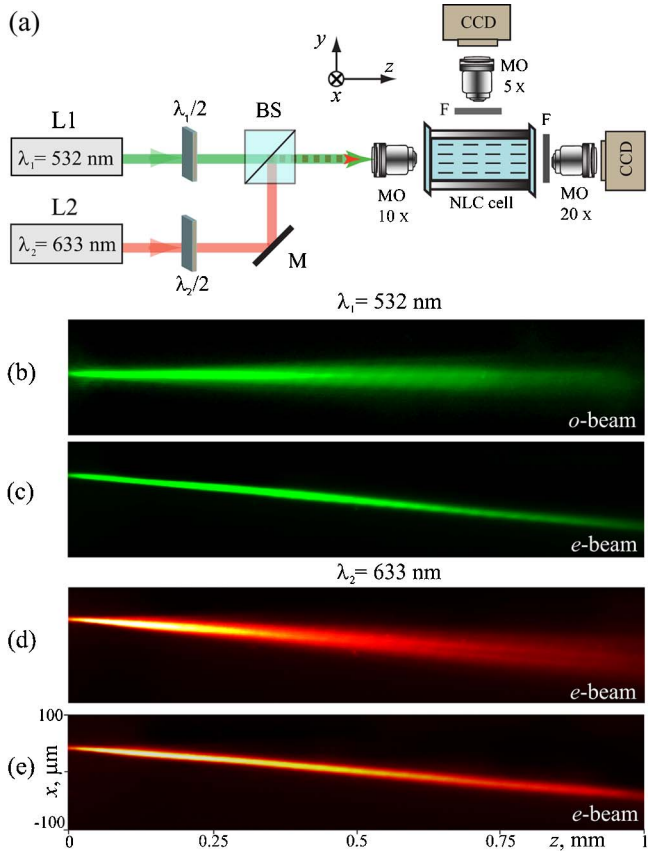

Fig. 1. (Color online) (a) Experimental setup: L1, L2, the green ($\lambda_1 = 532$ nm) and red ($\lambda_2 = 633$ nm) cw lasers; $\lambda/2$, half-wavelength plates; BS, beam splitter; M, mirror; MO, micro-objectives; F, filter; CCD, camera. Top view of (b) ordinary and (c)–(e) extraordinary beams: (b), (c) green beam ($P =$ 2 mW); (d) diffracting; (e) nematicon-guided red beam (power 82 μW).

whereas the e beam in Fig. 1(c) is self-trapped while walking off at an angle ~5° with respect to **k**. The e-signal beam (red, $\lambda_2 = 633$ nm) is copolarized and launched collinearly with the green beam, resulting in either diffraction without nematicon [Fig. 1(d)], or guided-wave confinement by nematicon [Fig. 1(e)]. The input power of the signal red beam in all experiments was 82 μW.

Noteworthily, the nematicons are generated in a uniaxial liquid medium subject to slow dynamics [17] and instabilities [18,19], where birefringence-induced walk-off is power sensitive [19,20] and nonlocality leads to beam breathing [9,21]. In the absence of an external bias, as in our configuration, these effects result in a bent nonuniform waveguide with fluctuations on a time scale smaller than the inverse maximum frame rate of our camera (25 fps). Corresponding changes in modal profiles and the time-dependent mode mixing [16] demand for temporal averaging of output images recorded during data acquisition, typically 40 frames at 4 fps. Therefore, we define mode HWHMs, $w_{x,y}$, as two half-sizes of a rectangle enclosing the contour line of averaged intensity profile at the half-peak level.

Figure 2 shows the experimental results for a green nematicon [Fig. 2(a)] and a weak red fundamental H_{00} mode colaunched at the input [Figs. 2(b)–2(d)]. At low nematicon power ($P < 0.9$ mW), the self-focusing reduces the waist in the green and the corresponding size of the guided mode in the red, until a nematicon is generated for $P > 0.9$ mW [Fig. 2(a)] and the red signal becomes a guided mode [Fig. 2(b)]. The shaded region in Fig. 2(b) marks the existence of a stable H_{00} guided mode, with the typical averaged output transverse profile displayed in Fig. 2(c). Further increases of nematicon power P lead to a soliton waveguide supporting more guided modes, with a stronger mixing and an output signal exhibiting a multihump profile, as in Fig. 2(d). The latter transition for $P > 3$ mW is accompanied by an increase in HWHM for the red signal, as is apparent in Fig. 2(b), whereas the nematicon maintains its robust structure [Fig. 2(a)]. Clearly, the nonlinear refractive index potential gets higher and wider with nematicon excitation, inducing a multimoded channel waveguide where a complex pattern appears owing to superposition and mixing of guided modes [16].

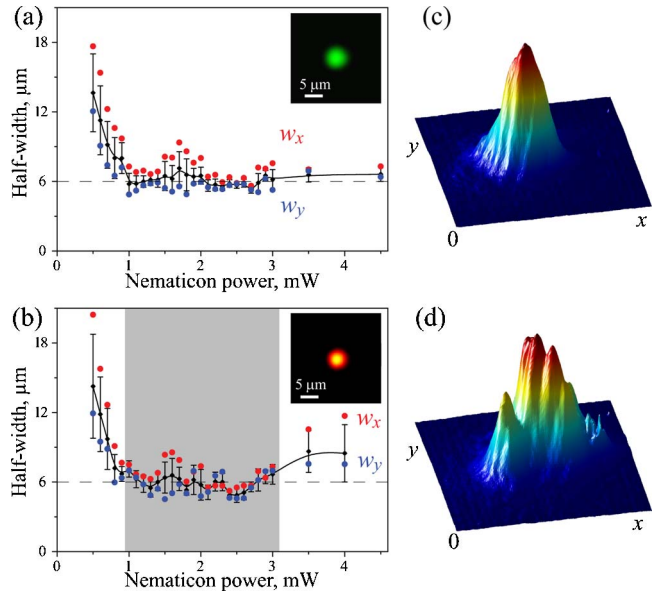

Fig. 2. (Color online) Beam HWHM $w_{x,y}$ (dots) of (a) green nematicon and (b) red fundamental guided mode; the mean radius and standard deviation of a circular fit are shown with the solid curve and error bars. The shaded area in (b) marks the region of stable guiding; the insets show input beams. (c), (d) Averaged intensity distributions of the mode guided by nematicons of powers (c) 1.5 mW and (d) 4mW; the window is 67.3 μm × 67.3 μm.

To excite the first-order mode in the soliton-induced waveguide, we insert a thin glass plate in front of half of the signal beam and tilt it, introducing a π phase jump, in order to reproduce the phase profiles of H_{10} and H_{01} modes; see the insets in Figs. 3(b)–3(d). The HWHM of both modes versus nematicon excitation [Figs. 3(a)–3(c)] exhibit (shaded) regions of stable guidance, with averaged profiles shown in Figs. 3(b)–3(d). At low excitation powers, the strong diffraction of the signal beam is limited only in the y direction by the cell boundaries; thus, $w_y < w_x$. At variance with soliton waveguides in photorefractive crystals, subject to a directional bias [8], both dipolelike modes coexist in the same interval of excitations, $1.2 < P[\text{mW}] \leq 2$, suggesting that the role of the cell boundaries and the related index anisotropy [22] are minimal in this case. Using two glass plates, we generate

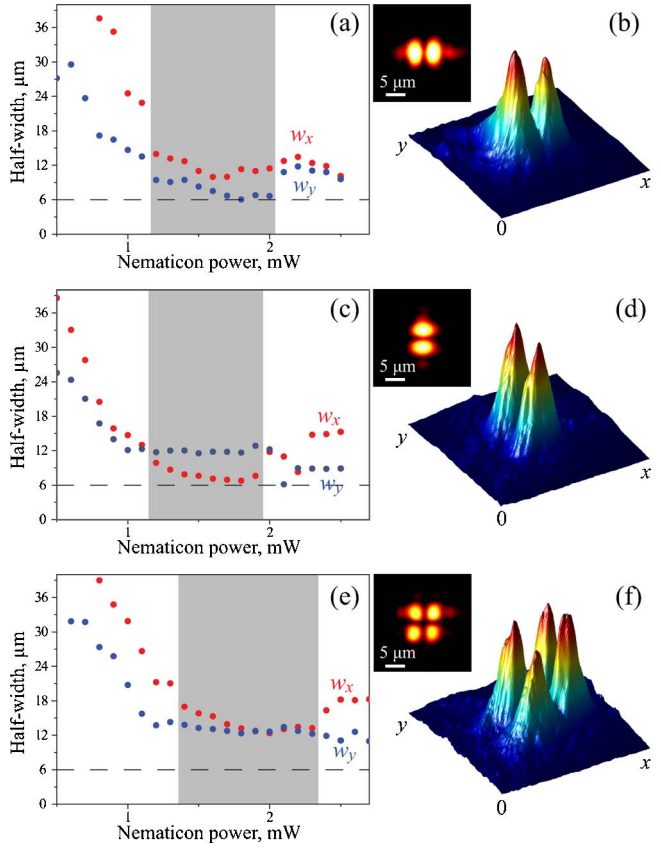

Fig. 3. (Color online) Experimental results for (a), (b) H_{10}; (c), (d) H_{01}; and (e), (f) H_{11} modes launched in the red at the input and guided by a nematicon. (a), (c), (e) HWHM versus nematicon power P; the shaded regions indicate domains of stable guiding. (b), (d), (f) Averaged intensity distributions for $P = 1.5$ mW; the windows are 67.3 μm × 67.3 μm in (b), (d) and 80.7 μm × 80.7 μm in (f). The insets show input profiles.

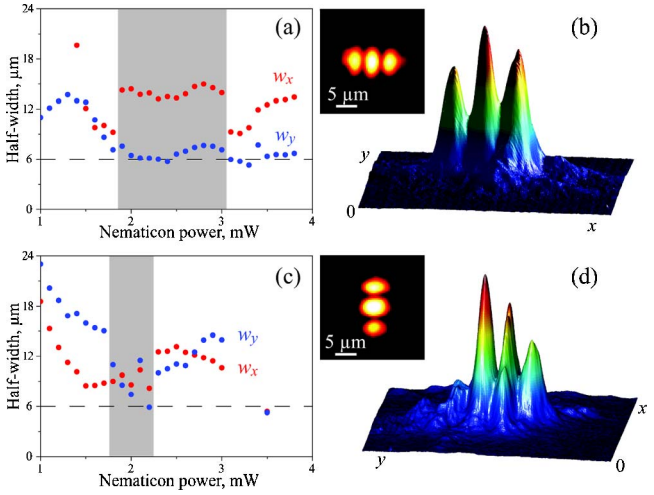

Fig. 4. (Color online) Experimental results at the cell output for (a), (b) H_{20} and (c), (d) H_{02} modes guided by a nematicon. (a), (c) HWHM versus nematicon power P. (b), (d) Averaged intensity outputs for $P = 2$ mW in the windows 80.7 μm× 80.7 μm; the insets show input profiles.

and launch the red signal H_{11} mode, as shown in Figs. 3(e) and 3(f). The HWHM of this mode in both x and y corresponds well to the size of H_{10} and H_{01} modes above, ~12 μm, approximately twice wider than the nematicon (see dashed lines). As expected, the (shaded) stable domain for H_{11} is shifted toward higher powers with $1.4 < P[\mathrm{mW}] < 2.3$.

Finally, Fig. 4 shows the experimental results for H_{20} and H_{02} modes, generated with two glass plates. The H_{20} mode displays a relatively broad domain of stable existence, $1.8 < P[\mathrm{mW}] < 3$. Its HWHM $w_x \simeq 15$ μm is nearly three times larger than the nematicon. In sharp contrast, the vertically oriented H_{02} mode [Fig. 4(d)] is only quasi-stable in a narrow domain, $1.7 < P[\mathrm{mW}] < 2.2$, owing to the (anisotropic) role of the cell boundaries at $y = 0, L$ with fixed director orientation, and despite the fact that its total width, $2w_y < 24$ μm, is much smaller than the cell thickness $L = 100$ μm. It follows that the order of the supported guided modes is limited from above not only by the nematicon power and mode-mixing process but also by the boundary-induced anisotropy [22]. For H_{mn} with $(m, n) \leq 1$, the nematicon waveguides can be considered isotropic and circularly symmetric.

In conclusion, we have shown experimentally that the waveguides induced by spatial solitons in unbiased NLCs can support various copolarized guided modes. Multimode waveguides exist in well-defined regions of excitation powers. The confinement of several guided modes in self-induced waveguides is potentially useful for soliton-based optical switches, interconnects, and all-optical processing.

The authors acknowledge the Australian Research Council for financial support and thank W. Krolikowski and A. Alberucci for useful suggestions.

References

1. Yu. S. Kivshar and G. P. Agrawal, *Optical Solitons: From Fibers to Photonic Crystals* (Academic, 2003).
2. M.-F. Shih, M. Segev, and G. Salamo, Opt. Lett. **21**, 931 (1996).
3. M. Peccianti, G. Assanto, A. De Luca, C. Umeton, and I. C. Khoo, Appl. Phys. Lett. **77**, 7 (2000).
4. J. Petter and C. Denz, Opt. Commun. **188**, 55 (2001).
5. M. Peccianti and G. Assanto, Opt. Lett. **26**, 1690 (2001).
6. J. F. Henninot, M. Debailleul, R. Asquini, A. d'Alessandro, and M. Warenghem, J. Opt. A **6**, 315 (2004).
7. Ya. V. Izdebskaya, V. G. Shvedov, A. S. Desyatnikov, W. Krolikowski, and Yu. S. Kivshar, Opt. Lett. **35**, 1692 (2010).
8. J. Petter, C. Denz, A. Stepken, and F. Kaiser, J. Opt. Soc. Am. B **19**, 1145 (2002).
9. C. Conti, M. Peccianti, and G. Assanto, Phys. Rev. Lett. **92**, 113902 (2004).
10. X. Hutsebaut, C. Cambournac, M. Haelterman, J. Beeckman, and K. Neyts, J. Opt. Soc. Am. B **22**, 1424 (2005).
11. J. F. Henninot, J. F. Blach, and M. Warenghem, J. Opt. A **9**, 20 (2007).
12. X. Hutsebaut, C. Cambournac, M. Haelterman, A. Adamski, and K. Neyts, Opt. Commun. **233**, 211 (2004).
13. J. Beeckman, K. Neyts, P. J. M. Vanbrabant, R. James, and F. A. Fernandez, Opt. Express **18**, 3311 (2010).
14. M. Mitchell and M. Segev, Nature **387**, 858 (1997).
15. M. Peccianti and G. Assanto, Opt. Lett. **26**, 1791 (2001).
16. A. M. Snyder and J. D. Love, *Optical Waveguide Theory* (Chapmen and Hall, 1983).
17. J. Beeckman, K. Neyts, X. Hutsebaut, C. Cambournac, and M. Haelterman, IEEE J. Quantum Electron. **41**, 735 (2005).
18. C. Conti, M. Peccianti, and G. Assanto, Opt. Lett. **31**, 2030 (2006).
19. Ya. V. Izdebskaya, V. G. Shvedov, A. S. Desyatnikov, W. Z. Krolikowski, M. Belic, G. Assanto, and Yu. S. Kivshar, Opt. Express **18**, 3258 (2010).
20. A. Piccardi, A. Alberucci, and G. Assanto, Appl. Phys. Lett. **96**, 061105 (2010).
21. M. Peccianti, A. Fratalocchi, and G. Assanto, Opt. Express **12**, 6524 (2004).
22. C. Conti, M. Peccianti, and G. Assanto, Phys. Rev. E **72**, 066614 (2005).